Experimental study on multiphoton ionization of Ar with high intensity short laser pulses

Xiaoyin Zhang (张晓吟)[1,2], Wei Quan (全 威)[1*], Yang Wang (王 阳)[1,2], Huipeng Kang (康会鹏)[1,2], Hongping Liu (刘红平)[1], and Xiaojun Liu (柳晓军)[1]**

[1]*State Key Laboratory of Magnetic Resonance and Atomic and Molecular Physics, Wuhan Institute of Physics and Mathematics, Chinese Academy of Sciences, Wuhan 430071, China*

[2]*Graduate University of Chinese Academy of Sciences, Beijing 100049, China*

[*]*E-mail: charlywing@wipm.ac.cn;* [**]*e-mail: xjliu@wipm.ac.cn*

Received May 14, 2009

We present high resolution photoelectron energy spectra from multiphoton ionization (MPI) of Ar subject to laser pulses with wavelength of 400 nm, pulse duration of 35 fs, and maximum intensity of 5×10^{13} W/cm^2. Ionizations into Ar^+ $^2P_{3/2}$ and $^2P_{1/2}$ channels are observed and distinct resonance structures are found in both ionization channels. The intensity dependence of the resonance structures is explained in terms of the mechanism of Freeman resonance, i.e., transient resonances of alternating current (AC) Stark-shifted Rydberg states at specific intensities within the laser pulse.

OCIS codes: 300.6350, 020.4180, 020.5780.

doi: 10.3788/COL20100803.0338.

The studies of multiphoton ionization (MPI) processes of noble gas atoms greatly advanced our understanding of atomic dynamics in ultrashort intense laser pulses over the past thirty years. In 1979, Agostini *et al.* found that a Xe atom might absorb more photons than required for ionization, a process coined as above-threshold ionization (ATI)[1]. In the earlier days, the pulse widths of the lasers were longer compared with the time during which the ionized electrons left the interaction region. Photoelectron energy spectrum at this long pulse regime exhibited a series of structureless peaks separated by one photon energy[2−6]. In 1987, Freeman *et al.* revealed that, as the pulse duration decreased, each ATI order in photoelectron energy spectrum shifted to lower energy and the individual ATI peaks broke up into narrow fine structures[7]. This phenomenon is named as Freeman resonance.

The appearance of Freeman resonance can be explained by multiphoton resonances between the ground state and the alternating current (AC) Stark-shifted Rydberg states. Within a strong laser field, the energy level of a Rydberg state, and the energy spacing between it and the ground state exhibit strong dependence on the laser intensity. Only at some specific laser intensities, for which the shifted energy spacing equals an integral multiple of the photon energy, Freeman resonance will occur and result in fine structures in photoelectron energy spectra. In parallel with the experimental observation of such multiphoton resonances, theoretical efforts have been paid and facilitated the understanding of this phenomenon. For example, a time-dependent theory of multiphoton ionization starting from Floquet ansatz was formulated by Potvliege *et al.*[8] Within this framework, the authors argued that the resonance structure in ATI spectrum came through the electron jumping from one dressed-state energy eigenvalue curve to another. Hansch *et al.* employed a simple multiphoton Landau-Zener theory to analyze the evolution of the resonances with laser intensity[9]. Very recently, Guo *et al.* provided an *ab initio* theoretical explanation for the occurrence of Freeman resonance and proved its strong dependence on the laser intensity, by formulating a closed-form expression for the quasienergies of simplified two-level atom interacting with a monochromatic laser field[10,11].

So far, most experimental studies on short-pulse MPI, in which Freeman resonance plays a key role in understanding the dynamics, have been performed on atomic Xe. Therein, many strong-field processes, such as resonance and nonresonant processes[9,12], ionization channels into different ionization limits, e.g., Xe^+ $^2P_{3/2}$ and $^2P_{1/2}$ limits[13], and channel switching effects[9,12], have been revealed. In contrast, only little work has been done with Ar in the intensity range around 10^{13} W/cm^2, where MPI is the dominant ionization mechanism. Recent experimental study on short-pulse MPI of Ar with 800-nm, 100-fs laser pulses has been performed with the help of a momentum spectrometer[14]. This experiment shows exclusively ionization into the ionic $^2P_{3/2}$ channel and resonance enhancements by bound states with $3p^5$ $^2P_{3/2}$ ion core character. On the other side, a poor energy resolution inherent with the momentum spectrometer prevents a clear identification of the resonance structures, which plays a major role in understanding the MPI processes of Ar.

In this letter, we present high resolution photoelectron energy spectra from MPI of Ar exposed to 400-nm, 35-fs laser pulses in the intensity range of 10^{13} W/cm^2. Our experimental data show ionizations into Ar^+ $^2P_{1/2}$ channel, in addition to $^2P_{3/2}$ channel that was observed in previous study with laser pulses of 800 nm[14]. Moreover, our results reveal unambiguously transient resonances in a MPI process leading to both the $^2P_{1/2}$ and $^2P_{3/2}$ ionization channels. The evolution of the photoelectron energy spectra with the laser intensity can be understood with the mechanism of Freeman-type resonance.

 © 2010 Chinese Optics Letters

In our experiments, the ultrashort laser pulse was seeded from a commercial Ti:sapphire laser system (Mira Seed, Coherent) and amplified by a Ti:sapphire amplifier laser system (Lengend, Coherent). The ultrashort laser pulse output from the final stage of the laser system was centered at 800 nm. A 0.5-mm-thick beta barium borate (BBO) crystal was employed to produce second harmonics, which had a center wavelength of 400 nm and a pulse duration of 35 fs. The combination of a $\lambda/2$ wave plate and a polarizing cube was introduced to manipulate the laser intensity. An achromatic lens with 300-mm focal length was used to focus the laser beam within an ultrahigh vacuum (UHV) chamber to a spot. The photoelectron energy spectrum was measured with a field-free time-of-flight (TOF) spectrometer. The field-free flying length was around 470 mm and an energy resolution of about 20 meV at 1 eV was achieved with this spectrometer. Attention has been paid to keep the spectrometer against the stray magnetic field with μ-metal tube. The background pressure during experiments was kept below 10^{-6} Pa by a turbomolecular pump and a cryopump.

Figure 1 shows the short-pulse photoelectron energy spectra of Ar at 400 nm with three different intensities of 4.8×10^{13}, 3.4×10^{13}, and 2.8×10^{13} W/cm^2. The spectra cover the energy range of the two lowest ATI orders $n\hbar\omega$ and $(n+1)$ $\hbar\omega$ (n = 0,1, $\hbar\omega$ = 3.10 eV) separated by the straight vertical lines labeled by $(n+1)\hbar\omega$ (n = 0, 1). Before analyzing the measured spectra in detail and further understanding the intensity dependence of the spectra, we first give an overall description of the spectra based on two kinds of MPI processes, i.e., resonant and nonresonant processes, that contribute to the photoelectron energy spectra. For nonresonant ionization process, the atom is directly ionized after absorbing enough photons from the initial ground state. The final energy of the photoelectron emitted from this process depends on the laser intensity I and is given by

$$E_{\rm e}(I) = n\hbar\omega - [E^+ + U_{\rm p}(I)], \tag{1}$$

where n is the number of photons required to ionize the atom, E^+ is the energy threshold of the field-free ionization, and $U_{\rm p}(I)$ is the ponderomotive potential which can be calculated with

$$U_{\rm p}(I) = 9.33\times10^{-14}\times I\times\lambda^2, \tag{2}$$

where λ is the wavelength in the unit of μm. Note that for Ar, two different ionization channels, i.e., ionizations into Ar^+ $^2P_{3/2}$ and $^2P_{1/2}$ with thresholds E^+ of 15.76 and 15.93 eV, respectively, are present. The energy difference between the two thresholds is 0.17 eV. In Fig. 1, the dashed vertical lines labeled by $^2P_{3/2}$ and $^2P_{1/2}$ mark, according to Eq. (1), the energy $E_{\rm e}(0)$ that a photoelectron produced at zero intensity would have, after 6-photon absorption from the Ar ground state with the ion left in the state $^2P_{3/2}$ and $^2P_{1/2}$, respectively. The $^2P_{3/2}+\hbar\omega$ and $^2P_{1/2}+\hbar\omega$ lines thus represent the energy of the electrons after 7-photon absorption from the ground state of Ar, i.e., 1-photon absorption above the ionization threshold. In the experiments, however, the photoelectrons are released at the intensity different from zero. We therefore mark the possible energy ranges of the photoelectron by the horizontal lines whose lengths are determined by the ponderomotive energy corresponding to the peak laser intensity employed in the spectra.

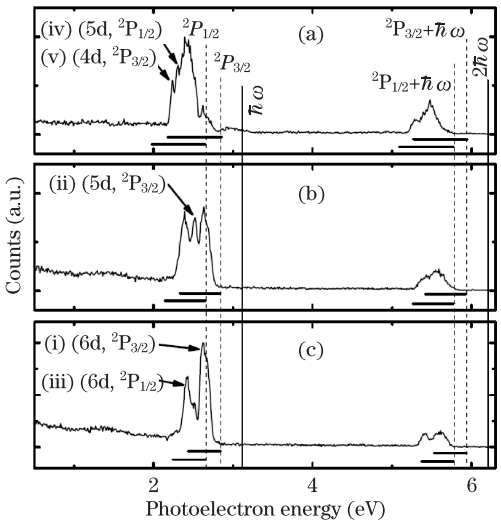

Fig. 1. Photoelectron energy spectra of Ar subject to intense laser pulses with wavelength of 400 nm, pulse duration of 35 fs, and peak intensities of (a) 4.8×10^{13}, (b) 3.4×10^{13}, and (c) 2.8×10^{13} W/cm^2.

According to Eq. (1), electrons emitted into the ionization channels $^2P_{3/2}$ and $^2P_{1/2}$ should appear within the energy ranges delimited by the horizontal lines starting from the vertical lines labeled by $^2P_{3/2}$ ($^2P_{3/2}+\hbar\omega$) and $^2P_{1/2}$ ($^2P_{1/2}+\hbar\omega$), respectively. Indeed, as shown in Fig. 1, the electrons are detected only within these energy intervals.

In addition, the groups of photoelectrons in this energy range show distinct resonance structures. These structures can be ascribed to a resonant multiphoton ionization via highly excited Rydberg states of Ar that AC Stark shifts into resonance at a specific intensity within the laser pulse (i.e., Freeman resonance). In the case of a resonant $(m+1)$-photon ionization process, the final kinetic energy of the photoelectron observed in the spectra is given by

$$E_{\rm e} = \hbar\omega - (E^+ - E_{\rm Ryd}), \tag{3}$$

where $E_{\rm Ryd}$ is the field-free energy of the Rydberg state. Here we take the assumption that the AC Stark shift of the Rydberg state equals that of the ionization threshold, i.e., the ponderomotive energy $U_{\rm p}$. This is usually a good approximation for tightly bound atoms such as rare gas atoms[15]. Note that in this resonant case, the energy of the emitted photoelectron is independent of the peak laser intensity.

To help identify the relevant states that are responsible for the resonance structures in Fig. 1, we show schematically part of the field-free energy levels of Ar in Fig. 2 for the energy range of 14.6–15.5 eV, which possibly play a key role in explaining the resonances according to the selection rules. The horizontal line labeled by $5h\nu$ represents the Ar ground state dressed with 5 photons.

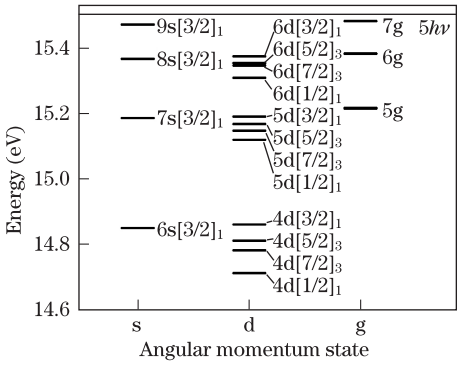

Fig. 2. Field free energy levels of Ar, which are relevant for interpreting the photoelectron energy spectra[16].

For the spectrum recorded at the lowest laser intensity of 2.8×10^{13} W/cm^2 (Fig. 1(c)), there are two distinct peaks at the energy positions of 2.43 eV (peak (iii)) and 2.62 eV (peak (i)). With the assumption that the highly excited Rydberg states of Ar shift nearly with ponderomotive potential $U_{\rm p}$ (about 0.42 eV), the possible candidates of the resonant states fall in the energy range from 15.50 ($5\hbar\omega$) to 15.08 eV ($5\hbar\omega$–$U_{\rm p}$). In this range, consideration of the angular momentum of the final state by 5-photon absorption from the Ar ground state $3p^6$ leads to possible candidates of the states 6g, 5g, 6d, 5d, 8s, and 7s. These are the only states that may shift into resonance at this peak laser intensity.

The energy position makes us assign peak (i) to the 6d state corresponding to the $^2P_{3/2}$ ionization channel. However we are not able to resolve the sub-levels within the 6d state manifold which consists of different total angular momentum levels. As shown in Fig. 2, the energy range of the 6d levels with different total angular momenta covers about 60 meV, and the small energy separation between sub-levels prevents us from clearly resolving them. This may also explain the rather broad width of the observed peak. On the other side, the broad width of this peak suggests that it should not come from the resonance with either s or g states, for which a rather narrow peak width would be expected[14].

Furthermore, we note that the energy separation between peaks (iii) and (i) is about 0.18 eV, which approximately equals the energy difference (0.17 eV) from the two ionization thresholds for $^2P_{3/2}$ and $^2P_{1/2}$, considering the energy resolution (about 20 meV) of the spectrometer. It suggests that peak (iii) may be relevant to peak (i) and produced by the ionic core admixture of different ionization channels. The electrons, after absorption of one more photon from the resonant 6d state, may be emitted with different energy as the corresponding ionic core may stay in two different final ionic states $^2P_{3/2}$ and $^2P_{1/2}$. This core admixture effect has been observed in short-pulse MPI of Xe at 526.5 nm[12]. Furthermore, it is found that, peak (iii) shows a similar dependence on laser intensity as the peak (i), we thus believe that peak (iii) comes from the 6d state corresponding to $^2P_{1/2}$ ionization channel due to ionic core admixture.

A closer inspection reveals that, at this lowest intensity, another rather weak peak (ii) between peaks (i) and (iii) appears at about 2.52 eV. This peak becomes prominent with the increase of the laser intensity, as shown in Fig. 1(b). We assign this peak to the 5d state. The fine structure of this state ranges from 2.45 to 2.53 eV in the kinetic energy spectra. If assuming an AC Stark shift nearly equal to the ponderomotive potential, the 5-photon resonance intensity for the 5d state is about 2.5×10^{13} W/cm^2. This state can thus be populated significantly at the laser intensity of 3.4×10^{13} W/cm^2, as shown in Fig. 1(b).

As the laser intensity increases further, as shown in Fig. 1(a), peak (ii) corresponding to the 5d state becomes dominant and peak (iii) looks like a shoulder of it, while peak (i), which is assigned to the state 6d corresponding to $^2P_{3/2}$ channel, becomes smaller. The change of the relative strength of these peaks may be explained in terms of the dependence on the laser intensity of the excitation probability of the excited states. The wavefunction overlap between the 6d state and the ground state should be smaller than that for the 5d state, resulting in a smaller excitation cross section for the former. Besides, the laser intensity required to resonantly excite 6d state is lower than that for the 5d state. Larger excitation cross section and higher resonant laser intensity will give rise to the prominent photoelectron yield from the 5d state.

Two more peaks, i.e., peaks (iv) and (v), are also present in Fig. 1(a). It is found that the energy difference between peaks (iv) and (ii), which is assigned to the 5d state, is very close to 0.17 eV, the energy separation of the two ionization thresholds. We thus assign this peak to the same state, 5d, but corresponding to $^2P_{1/2}$ ionization channel, due to the core admixture effect discussed above. While peak (v) is assigned to the state 4d, for which 5-photon resonance intensity is around 4.5×10^{13} W/cm^2. This state can only be populated and contribute to the spectrum when the laser intensity is increased to 4.8×10^{13} W/cm^2.

For the spectra in the energy range of 5–6 eV, there exists another group of resonance structures, which corresponds to the first-order ATI series. These structures show a similar intensity dependence as their counterparts in the energy range of 2–3 eV. With the increase of the laser intensity, the groups of the structures shift to lower electron energy due to the fact that lower Rydberg states shift into resonances and contribute to the photoelectron yield. However, as the energy resolution of the TOF spectrometer decreases approximately with $E^{3/2}$, some of the resonance structures may not be distinguished within this order of ATI.

In conclusion, we have observed and analyzed the resonance structures in the low-energy photoelectron spectra from ATI of Ar subject to 400-nm short laser pulses. These resonance structures are tentatively identified as d-angular momentum states corresponding to both $^2P_{3/2}$ and $^2P_{1/2}$ ionization channels. The intensity dependence of the structures can be understood with the mechanism of transient resonances of AC Stark-shifted Rydberg states.

This work was supported by the National Natural Science Foundation of China (No. 10674153) and the Natural Science Foundation of Hubei Province (No. 2008CDB007).

References

1. P. Agostini, F. Fabre, G. Mainfray, G. Petite, and N. K. Rahman, Phys. Rev. Lett. **42,** 1127 (1979).
2. P. Kruit, J. Kimman, H. G. Muller, and M. van der Wiel, Phys. Rev. A **28,** 248 (1983).
3. M. Mittleman, J. Phys. B **17,** L351 (1984).
4. E. Fiordilino and M. Mittleman, J. Phys. B **18,** 4425 (1985).
5. P. H. Bucksbaum, M. Bashkansky, R. R. Freeman, T. J. McIlrath, and L. F. DiMauro, Phys. Rev. Lett. **56,** 2590 (1986).
6. T. J. McIlrath, P. H. Bucksbaum, R. R. Freeman, and M. Bashkansky, Phys. Rev. A **35,** 4611 (1987).
7. R. R. Freeman, P. H. Bucksbaum, H. Milchberg, S. Darack, D. Schumacher, and M. E. Geusic, Phys. Rev. Lett. **59,** 1092 (1987).
8. R. M. Potvliege and R. Shakeshaft, Phys. Rev. A **38,** 4597 (1988).
9. P. Hansch, M. A. Walker, and L. D. V. Woerkom, Phys. Rev. A **57,** R709 (1998).
10. D.-S. Guo, Y.-S. Wu, and L. V. Woerkom, Phys. Rev. A **73,** 023419 (2006).
11. D.-S. Guo, J. T. Wang, and Y.-S. Wu, Phys. Rev. A **77,** 025401 (2008).
12. V. Schyia, T. Lang, and H. Helm, Phys. Rev. A **57,** 3692 (1998).
13. H. Rottke, J. Ludwig, and W. Sandner, J. Phys. B **29,** 1479 (1996).
14. R. Wiehle, B. Witzel, H. Helm, and E. Cormier, Phys. Rev. A **67,** 063405 (2003).
15. P. Agostini, A. Antonetti, P. Breger, M. Crance, A. Migus, H. G. Muller, and G. Petite, J. Phys. B **22,** 1971 (1989).
16. T. Shirai, J. Sugar, and A. Musgrove, "Wavelengths and energy levels for all spectra of argon (Ar I through Ar XVIII)" http://physics.nist.gov/PhysRefData/ASD/levels_form.html (Apr. 20, 2009).